*International Journal of Engineering and Science Invention (IJESI)*
*ISSN (Online): 2319-6734, ISSN (Print): 2319-6726*
*www.ijesi.org ||Volume 12 Issue 10 October 2023 || PP 82-100*

# Comparison of Magnetized Silicon Oxide and Aluminum Oxide Nanofluids in Solar Desalination with Thermal Storage

S. Sami[1,2]

[1.] *Research & Development Department, TransPacific Energy, Inc, Las Vegas, NV, 89183, USA*
[2.] *Institute of Energy Systems, North Dakota University, Grand Forks, ND, 58202, USA*

***Abstract:***
*The magnetized nanofluid Silicon Oxide and Aluminum Oxide have been studied mathematically and numerically in solar desalination multistage flashing chambers using the PV-thermal solar collectors' concept. A mathematical formulation was written after mass and energy conservation balances using finite control volume and properties of magnetized $SiO_2$ and $A_2O_3$ nanofluids. The flashing process was examined in multiple chambers under various conditions including different solar radiations, brine flows, and concentrations, various magnetic field strengths, different irreversibility, and availabilities as well as flashing chamber conditions.*
*Higher solar radiation increases the flash flow produced. It is concluded that higher irreversibility was experienced when water was used as a base fluid. The irreversibility increase depends upon the type of nanofluid and its thermodynamic properties. Furthermore, higher concentration increases the availability at the last flashing chamber depending on the type of nanofluid and its thermodynamic properties. Also, the availability progressively decreased at the last flashing chamber. The higher the magnetic field forces the better the performance of nanofluids in the flashing chambers. The thermal energy accumulated during the thermal storage charging phase was significantly enhanced by using the magnetized nanofluid $SiO_2$. Finally, the model-predicted results compared well with experimental data published in the literature.*

***Keywords:***
*Desalination, flashing chamber, PV Thermal collectors, magnetized nanofluids, magnetic field, Numerical Model, validation.*

---

Date of Submission: 04-10-2023 Date of Acceptance: 16-10-2023

---

## I. Introduction:

Solar desalination is particularly important for locations where solar intensity is high and fresh water is scarce. Since thermal desalination is regarded as energy-intensive, seawater desalination and frac flow back water desalination require more energy than conventional water treatment due to the higher salt concentration [6,7]. Therefore, researchers are focusing on alternative renewable energy sources and technologies such as solar energy. It is believed that solar energy is the ultimate response to these limitations and can also provide thermal and electrical desalination systems. It was shown by references [5,6] that solar desalination can be achieved in areas where solar intensity is high and there is a lack of drinking fresh water.

An overview of present desalination status and freshwater demand, fuel requirements, solar energy availability, thermal desalination technologies, and solar thermal technologies has been presented in P. S. Bhambare et al. [7]. Conventional thermal desalination technologies and solar thermal technologies have been compared for the same capacity on a scale of 1 to 5 for various factors in the context of the Sultanate of Oman. Scheffler dish reflectors (SDR) are suggested as one of the most suitable options to be coupled with multi-effect desalination technology for small to medium-capacity decentralized-type plants. Parabolic trough collectors (PTC) coupled with Combined Cycle Gas Turbine (CCGT), or Open Cycle Gas Turbine (OCGT) plants would be a feasible solution for higher capacity desalination plants.

In the paper by Mahdi Shayanmehr and Hamed Mahdavi, [8], a novel modified model is presented for increasing the efficiency and performance of desalination systems. This suggested modification is based on a triple action. The first of these actions includes discovering the optimal location for the installation of solar still water. Increasing the contact surface of the water by spraying and keeping the saltwater in a wide solar still is a second approach for increasing the evaporation of water. In the end, a modern condensing system based on an innovative fog (water particle) trapper/harvester. This system includes fog fences, a cool water pipe loop based on the outdoor temperature, and forced-controlled airflow. Therefore, based on this method, a conceptual design

of solar still water desalination is modeled for the UAE. These results show that the efficiency of the proposed model is two times higher than the traditional method with the same cost.

Nannaronea et al. [9] presented a simulation model for the multiple-stage flash distillation, MSF process and was implemented within the Camel-ProTM Process Simulator. Several validation tests confirmed that his model is an efficient tool for MSF plants' design and the prediction of the most important parameters taking place in the MSF process.

Al-Fulaij's Ph.D. thesis [10] presented lumped parameter dynamic models for the once-through (MSF-OT) and the brine circulation (MSF-BC) processes and coded using the gPROMS modeling program. Results for both MSF-OT and MSF-BC in steady-state and dynamic conditions showed good agreement against data from existing MSF plants. Reference [10], provides a set of modular simulations of components that allow the creation of complex models used in the optimization of the full water desalination supply chain. The thesis included mathematical programming (MP) models that are solved by an external MP solver for Saudi Arabia.

A steady-state mathematical model for the multi-effect thermal vapor compression (ME-TVC) desalination system, the ME-TVC desalination system was developed by Amer [11], using Engineering Equations Solver (EES) to solve the model system. The Validation of the model against three commercial ME-TVC units was good. Also, this reference developed a MATLAB algorithm solution to solve model equations and different effects was tested to maximize the gain ratio of the process.

Reference [12], presented a model for the flashing process in the evaporation zone inside a flashing chamber with nanofluid-based solar collectors using a two-phase volume of fluid (VOF) formulation. The model investigates the effects of variations in the inlet brine flow rate and inlet brine temperature, for both finite and infinite flashing process classifications. The predictions were used to estimate MSF design factors such as the non-equilibrium temperature difference and flashing efficiency.

More recently, reference [13] review has focused on the role of nanofluids to improve heat transfer. He also reports and discusses the substantial role of nanofluids in enhancing the productivity and energy utilization efficiency of solar stills. Specifically, the mechanism of energy transfer between the nanoparticles and the base fluid. This includes both plasmonic and thermal effects. It was found that nanofluid use in small fractions enhanced thermal conductivity compared to base fluid alone. Alumina was found to be the most suitable nanoparticle used as nanofluid inside the solar stills due to its availability and lower cost. Still, other carbon nanostructures need to be investigated as they provide higher enhancement of thermal conductivity. Also, in this review, several aspects of energy utilization enhancement have been discussed, including innovative application techniques. The challenges of such integrated systems are addressed as well.

A conceptual design for a photovoltaic thermal (PV/T) solar panel has been developed and analyzed, to control the inherent temperature increase of PV cells to increase electrical efficiency [14-17]. The mathematical model for a multistage flash (MSF) desalination system with brine recirculation (BR) configuration has been developed and presented and the heat source for BR-MSF was described as a nanofluid-based direct absorption solar collector (DASC. The overall performance of the combined system was determined in terms of the gained output ratio referred to as (GOR).

More recently Sami [15] presented in his study solar flash desalination using PV-Thermal solar panels and nanofluids, modeling of the photovoltaic (PV)-thermal solar system to drive the multistage flashing chamber process and based on the mass and energy conservation balances written for finite control volume and integrated with the properties of the water and nanofluids. The nanofluids studied and presented herein are $Ai_2O_3$, CuO, $Fe_3O_4$, and $SiO_2$. He also studied the multi-flashing chamber process under various conditions. There was a piece of clear evidence that the higher the solar radiation, the higher the flash flow produced. The results also clearly showed that irreversibility was reduced by using nanofluid $Ai_2O_3$ at higher concentrations compared to water as a base fluid. The highest irreversibility was experienced when water was used as a base fluid and the lowest irreversibility was associated with nanofluid $SiO_2$. It was also shown that irreversibility increases depending on the type of nanofluid and its thermodynamic properties. Furthermore, higher concentration enhanced the availability at the last flashing chamber. However, the availability was progressively reduced at the last flashing chamber. Finally, the predicted numerical results compared well with experimental data.

Yang et al. [1], and Sami [18,19, 20] developed and reported on a hybrid solar panel to integrate photovoltaic (PV) cells onto a substrate through a functionally graded material (FGM) with water tubes cast inside, through which water serves as both heat sink and solar heat collector.

In the study by Kapil Garg et al. [18], a direct absorption solar collector (DASC) was used as a heat source for a multistage flash (MSF) desalination system having a once-through (OT) configuration, and these two systems are coupled using a counterflow type heat exchanger. This direct absorption collector was replaced by the surface-absorption-based collector to prevent the degradation of the thermal performance of the surface-absorption-based collector due to the high salinity of seawater and heated by the nanofluid flowing through the direct absorption collector. His study aimed to evaluate the thermal performance of the combined system which is represented by a quantity known as gained output ratio (GOR). It was found that the thermal performance or efficiency of the solar collector depends upon various parameters such as the thickness of the nanofluid layer

inside DASC, the length of the collector, the particle volume fraction of nanoparticles, and incident solar energy which will affect the performance of the MSF system.

In the research reported by reference [22], two identical solar stills were designed and constructed to investigate the effect of adding copper and aluminum oxide nanoparticles on the quantity of water produced by solar desalination. The two solar stills were installed side by side, and measurements were recorded simultaneously from both stills. The nanoparticles were added to one still, each at one time but at different concentrations. Data and weather conditions were recorded and solar radiation. It was found that the addition of nanoparticles increases the amount of condensate. The most efficient concentrations were found to be 0.4% of Al2O3 and 0.6% of CuO. An increase in the efficiency of the still equals 7.8%, and 9.62% was recorded. Furthermore, it was found that CuO has a more pronounced effect on the condensate than $Al_2O_3$ at all concentrations except at 0.4% concentration.

Further to the aforementioned literature review, very limited research work has been published on the use of nanofluids in the desalination process and using multistage flashing (MSF) chamber process modeling and simulation of seawater brine. Thermal and membrane desalination reported in the literature were only focused on the evaporation processes using steam. The novel concept presented in this paper for the MSF implements PV-Thermal solar panels using hot heat transfer fluid with magnetized nanofluids in the MSF process. Therefore, this research has been undertaken to study the impact of solar energy and magnetized nanofluids on the solar desalination process. The main objective of this research work is to develop and present mathematical and numerical modeling on the use of magnetized nanofluids and PV-thermal solar to drive the multistage flashing chamber thermal process. The model proposed was based on the mass and energy conservation equations of the flashing process integrated with the vapor and nanofluids' thermal and thermophysical properties at different volume fractions as well as solar radiation. The nanofluid studied hereby is $SiO_2$ and compared to nanofluid $Ai_2O_3$ as a reference-base well reported in the literature at different conditions. In this paper, the process of multistage flashing using PV-Thermal solar panels and magnetized nanofluids has been analyzed under different conditions of seawater (brine) salt concentration, brine flows, temperatures, and nanofluids concentration as well as solar radiations.

**Numerical Modeling:**
**PV model**

The solar photovoltaic panel is constructed of various modules and each module consists of arrays and cells. The dynamic current output can be obtained as follows [15-17].

$$I_P = I_L - I_o\left[exp\left(\frac{q(V+I_PR_S)}{AkT_C} - \frac{V+I_PR_S}{R_{sh}}\right)\right] \quad (1)$$

The AC power of the inverter output P(t) is calculated using the inverter efficiency $\eta_{inv}$ , output voltage between phases, neutral $V_{fn}$, and for single-phase current $I_o$ and $cos\varphi$ as follows.

$$P(t) = \sqrt{3}\,\eta_{inv}V_{fn}I_o\,cos\varphi \quad (2)$$

Interested readers in the AC power of the inverter output can consult Sami [15].

**PV-Thermal model:**
This model assumes that all PV cells behave the same, and it is an extension of the work presented by Sami and Campoverde [17] that the thermal heat absorbed by the PV solar cell can be calculated by the following equation.

$$Q_{in} = \alpha_{abs}GS_p \quad (3)$$

Were.
$\alpha_{abs}$: Overall absorption coefficient
G: Total Solar radiation incident on the PV module
$S_p$: Total area of the PV module

Meanwhile, the PV cell Temperature is computed from the following heat balance as per Sami and Martin [18].

$$mC_{p\_module}\frac{dT_C}{dt} = Q_{in} - Q_{conv} - Q_{elect} \quad (4)$$

Where.
$T_C$: PV Cell Temperature
$mC_{p\_module}$: Thermal capacity of the PV module

t: time
$Q_{in}$: Energy received due to solar irradiation,
$Q_{conv}$: Energy loss due to Convection
$Q_{elect}$: Electrical power generated.
Interested readers in the detailed calculations of the terms of the above equation are advised to consult references [15, 17, 18].

**Multistage Flashing Chamber Model:**
In the multistage flashing chamber thermal (MSF) process the brine is preheated by the magnetized nanofluid flow circulating in the PV-thermal loop where the dissipated heat from the PV solar panel is absorbed, as shown in the Figure.1 The flashing process occurs in the flashing chamber where the flashed vapor is generated and condensed on the heat exchanger cooled down by the incoming brine flow. The distilled condensed vapor is collected, and the brine flow is circulated to the next flashing chamber where the same flashing process is repeated for each flashing chamber. The numerical model hereby is considered for each discrete control volume with constant volume, therefore, by applying the first law of thermodynamics to each control volume, the mass balance, and energy balance across the flashing chamber can be given by the following equations respectively [7,15,32].

$$\Sigma m_{in} - \Sigma m_{out} = 0 \quad (5)$$

$$\Sigma e_{in} - \Sigma e_{out} = 0 \quad (6)$$

Where; $m$ and $e$ are the mass and energy entering and leaving the flashing chamber control volume.

The brine seawater mass balance across the preheater is.

$$m_{Bi} - m_{Bo} = 0 \quad (7)$$

Where $m_{CBi}$ and $m_{Bo}$ is the brine mass flow entering and leaving the preheater, respectively.

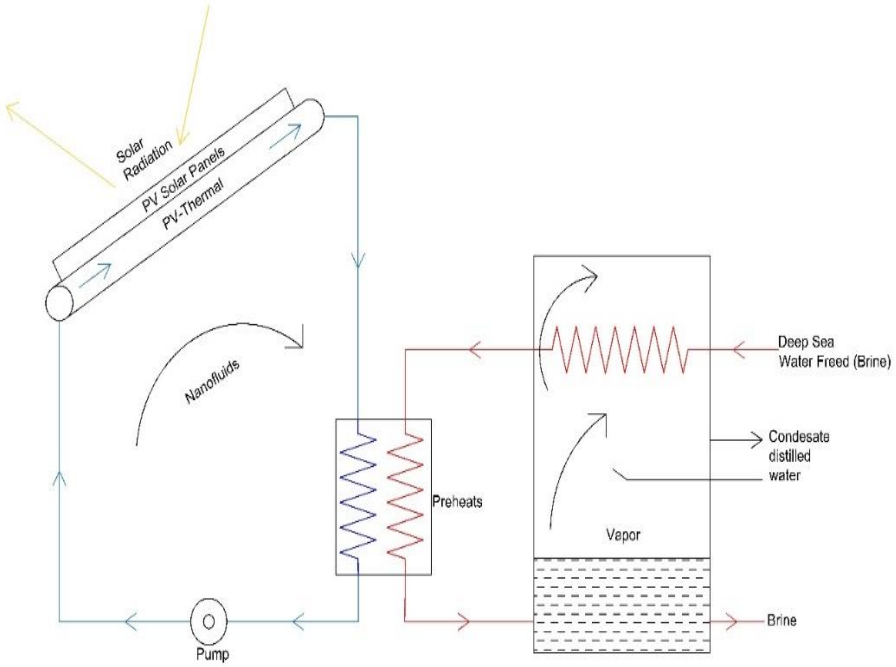


Figure 1 PV-Thermal integrated Flashing Chamber process.

The brine concentration entering and leaving is given by the mass balance equation.

$$m_{Bi}S_{Bi} - m_{Bo}S_{Bo} = 0 \quad (8)$$

The distilled condensed mass balance is.

$$m_{Co} - m_{Ci} - m_{Dbrine} = 0 \quad (9)$$

Where, $m_{Dbrine}$ is the distilled mass of vapor condensed as per Figure 1
The preheater energy balance is.

$$(m_{Dbrine} + \gamma m_{Bi})\Delta H_{evap} - m_{Bi}Cp_{brine}(T_{CBo} - T_{CBi}) = 0 \quad (10)$$

Where the distillate flashing fraction$\gamma$;

$$\gamma = \frac{Cp_{cond} * DT_{Stage}}{\Delta H_{evap}} \quad (11)$$

Where, $DT_{Stage}$ and $\Delta H_{evap}$ are the stage temperature difference and heat of evaporation, respectively.

**Nanofluid Heat Transfer Fluid**

The thermophysical, thermodynamic, and heat transfer properties of nanofluids are determined in terms of specific heat, thermal conductivity, viscosity, and density using the law of mixtures and the volumetric concentration of the nanoparticles as per the following equation [15, 17. 18].

$$\alpha_{\text{total}} = \alpha_{\text{particles}} + \alpha_{\text{base fluid}} \quad (12)$$

Where α represents the thermophysical property of a particular nanofluid.

The nanofluid thermal and thermophysical properties, $\alpha_{total}$, can be calculated as follows.

$$\alpha_{\text{total}} = \alpha_{\text{base fluid}} + \alpha_{\text{particles}} .(\Phi) \quad (13)$$

Where Φ represents the nanoparticles' volumetric concentration.

The thermal conductivity to thermal diffusivity and density of the nanofluids are related as follows [16-18}.

$$\lambda = \alpha\ \delta\ C_p \quad (14)$$

Where Cp is the specific heat, α is the thermal diffusivity, ʎ and ρ represent the thermal conductivity and density, respectively.

Interested readers in further details about the calculations of the nanofluid's thermophysical and thermodynamic properties are advised to consult references [16-18, 19-20, 22-24]. These references discuss the impact of the nanofluids concentrations on the thermophysical properties of the said nanofluids. Moreover, the scope of this study is to discuss the MSF process using the PV-Thermal with magnetized nanofluids as heat transfer fluids.

**Magnetized Nanofluids***:*

Equations (12) through (14) can be used to determine other thermophysical properties such as α is the thermal diffusivity, ʎ, and ρ represent the thermal conductivity and density as different magnetic forces Gauss published in the literature properties ([20] through [26]) as a function of the properties outlined in the Table.1

Table 1: Thermophysical Properties of magnetized nanofluids

| | **$Ai_20_3$** | **CuO** | **Fe304** | **$SiO_2$** |
|---|---|---|---|---|
| **$C_{p\ nf}$** | b = 0.1042a + 6226.5 | b = 0.2011a + 5730.8 | b = 0.8318a + 4269.8 | b = 0.6187a + 4293.2 |
| **$K_{nf}$** | b = 2E-05a + 1.4888 | b = 5E-05a + 1.3703 | b = 0.0002a + 1.0209 | b = 0.0001a + 1.0265 |
| **h** | b = 0.0031a + 73.092 | b = 0.0031a + 73.073 | b = 0.003a + 73.225 | b = 0.003a + 73.231 |

Where "b" represents the nanofluid-specific property and "a" is the magnetic field force in Gauss. $C_{pnf}$, Knf, and h are the specific heat, thermal conductivity, and heat transfer coefficients of nanofluids.

Finally, the Availability and Irreversibility of the flashing process are presented in the following, Sami [15].

$$A_q = \Sigma(1 - T_{amb}/T_J)\ Q_J \quad (15)$$

Where $A_q$ is the flow availability changes under steady-state conditions per stage and is the availability transfer due to $Q_J$, *the* heat transfer between the control volume and its surroundings. $T_{amb}$ *and* $T_j$ are the ambient temperatures and the Flashing chamber temperature, respectively.

The availability destruction i.e., irreversibility in the process per stage can be determined from the following.

$$I_j = T_{amb}\ x\ S_J \quad (16)$$

Where the $S_j$ represents the entropy of the flashing process at each stage

**Thermal Storage:**

The model presented hereby is an extension of the research work by Sami [30 and 31] and is based on the assumptions that the PCM is homogeneous and isotropic, HTF is incompressible, and it can be considered a Newtonian fluid, The solid and liquid phases have sensible heat additions and the mushy has latent heat addition. The conservation equations and heat transfer equations were written for each element/control volume of the PCM as follows for each of the phases of from solid, mushy, and liquid phases. The heat released by the heat transfer fluid HTF by each tube can be written as follows, [30,31],

$$\rho_{PCM} V_{PCM} Cp_{PCM} \frac{\Delta T_{PCM}}{\Delta t} = Qtub = m_w Cp_w \Delta T_w \quad (17)$$

The heat balance for the heat exchanger tube in the tank can be as follows.

$$(T_{in} - T_{out}) Cp_w m_w = 2\pi Rlh\left(T_{in} - T_{sfc}\right) \quad (18)$$

Where the heat transfer coefficient is approximated as [29].

$h = \frac{K_w}{D_H} b_2 Re^n$ and $Re = \frac{m_w D_H}{\mu A_f}$

And,

$Re$, Number-Reynolds, and is $Re = \frac{m_w D_H}{\mu A_f}$

**Charge phase:**

During the charging phase, the water mass flow rate can be calculated from the heat released by the solar radiation, The mass flow rate of water-based nanofluid:

$$m_w = \frac{GA_{Panel}}{1000 \times \cdot Cp_w \cdot \Delta T_w \cdot n} \quad (19)$$

**Solid phase**

$$T_{PCM_{m+1}} = T_{PCM_m} + \frac{m_w Cp_w \Delta T_w}{\rho_s V_{PCM} Cp_s} \Delta t \quad (20)$$

**Mushy phase:**

$$\gamma_{m+1} = \gamma_m + \left(\frac{m_w Cp_w \Delta T_{w,mushy}}{\rho_L V_{PCM} h_L}\right) \Delta t \quad (21)$$

**Liquid phase:**

With the finite-difference formulation of the time derivative, the PCM liquid temperature can be calculated as.

$$T_{PCM_{m+1}} = T_{PCM_m} + \frac{m_w Cp_w \Delta T_w}{\rho_L V_{PCM} Cp_L} \Delta t \quad (22)$$

**Discharge phase:**

During the discharge process phase, the change material experiences a phase change from liquid to mushy and solid while yielding heat that is absorbed during the charging process. The nanofluid-based water mass flow rate of heat transfer fluid during the discharge process can be calculated by ]29].

$$m_w = \frac{Q_{Charging}}{Cp_w \cdot \Delta T_w \cdot n} \quad (23)$$

Therefore, the total heat absorbed during the charging process by the phase change material during solid, mushy, and liquid phases is:

$$Q_{Charging} = m_{PCM}(Cp_s \Delta T_s + h_L + Cp_L \Delta T_L) \cdot n \quad (24)$$

Where:

$m_{pcm}$: mass of PCM per finite different element

**NUMERICAL PROCEDURE:**

The mass and energy equations (1 through 24) that take place during the flashing chamber process. are numerically solved as per the logical flow diagram in Figure 2. The calculation starts with the input of the parameters of the PV-Thermal solar panel, thermal tubes, desalination chamber parameters, nanoparticle $SiO_2$, and compared to $Ai_2O_3$, and heat transfer fluid. The system equations have been integrated and solved using the finite-difference formulations to determine the behavior of the process at each flashing chamber. Further, the thermophysical properties and the heat transfer characteristics of the base fluid, water, and magnetized nanofluids at different concentrations and different magnetic field forces, are determined to solve the mass and energy in the flashing chamber control volume. Iterations were performed using MATLAB iteration techniques until a converged solution was reached with less than 0.05. Finally, the individual and hybrid system efficiencies, availability, and irreversibility which represent the availability destruction in the process were calculated.

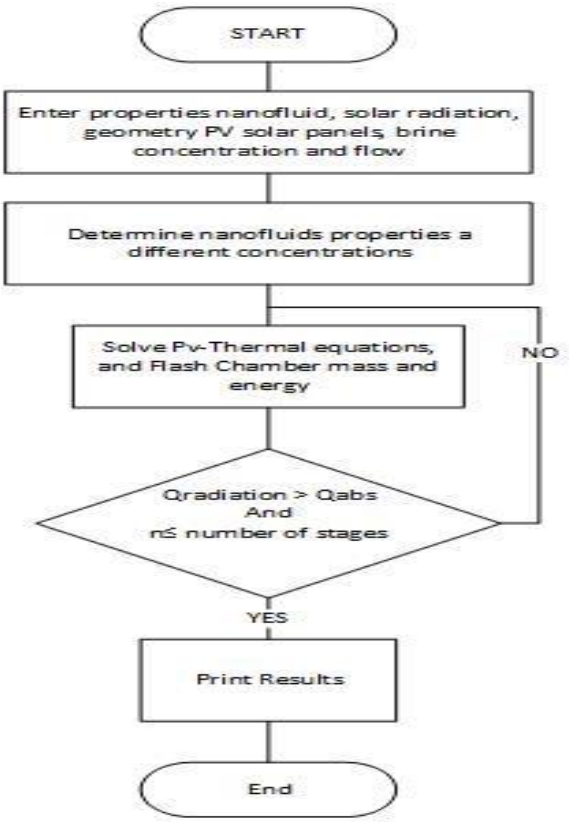


Figure 2 Logic diagram for the numerical solution.

## II. DISCUSSION AND ANALYSIS:

The system of equations (1) through (24) has been numerically solved in finite-difference formulation for predicting the desalination flashing process using nanofluids at different concentrations and water as base heat transfer fluid.

Equations (1) through (4) have been solved to predict the PV dynamic total power generated and efficiencies, in terms of the key important parameters of a photovoltaic-thermal solar panel hybrid system. As reported and discussed by Sami ([16] through [18]), it is evident from the results presented on the dynamic PV-Thermal studies that the higher the solar radiations the higher the thermal and hybrid efficiencies and the hybrid efficiency exhibits lower values than the thermal efficiency of the heat exchanger welded under the PV solar panels due to the PV solar panel efficiency is significantly lower than the thermal efficiency of the heat exchanger. Also, it was reported by Sami ([16] through [18]), that the higher the solar radiation the accelerated increase in the PV cell temperature, and subsequently, the higher the solar radiation the higher the PV power and PV amperage. Thereafter, the designer of the PV panel and its cell temperature must take into consideration solar radiation as well as the ambient conditions. Also, Sami [20-22,32] reported on nanofluids, such as $Ai_2O_3$ CuO, Fe3O4, and $SiO_2$, and PV-Thermal efficiency is enhanced with higher concentrations at constant solar radiation. It was assumed that ten flashing chambers were used, and the brine flow heats up in the heat transfer fluid preheater as shown in Figure. 1. A salt concentration of 5% was used in the brine flow and 60 F ambient temperature. Besides, 100 PV solar panels were assumed with 300 watts per PV solar panel. Solar radiation was taken as 500 w/m2, 750 w/m2, 1000 w/m2, and finally 1200 w/m2.

Since nanofluid Ai2O3 is one of the most common nanofluids studied and reported in the literature, Figures 3 and 4 were established at 500 W/m2 solar radiation to compare and demonstrate the impact of the key parameter in the study: the magnetic field in Gauss on the nanofluids $Ai_2O_3$, and $SiO_2$ and water, at different Gauss varying from 1000 through 3000, and different temperatures, respectively. $Ai_2O_3$ CuO, Fe3O4, and $SiO_2$

Examining the results presented in Figures 3 and 4, these suggest that the higher the magnetic field force nanofluid concentration as a heat transfer fluid, the lower the salt % in the flashed flow leaving and the PV thermal fluid temperatures, the higher thermal flashed flow rate at 500 W/m2. Also, the results showed that the $SiO_2$ outperforms the $Ai_2O_3$ and water. Also, Figure. 4, shows higher heat transfer fluid temperatures increase the brine flow temperatures and the amount of the distilled water evaporated or flashed.

On the other hand, it can be seen from Figures 5 and 6 that the higher the solar radiation the higher the flashed flow. This can be attributed to the fact that higher solar radiation results in a higher temperature of the heat transfer fluid and the brine flow in the preheater entering the flashing chambers. Also, the higher the heat

transfer fluid temperatures the higher the brine flow temperatures and the higher the amount of distilled water evaporated or flashed.

Figures 7 and 8 display the changes in the flashed flow at each chamber, at different solar radiations, where the flashed flow is reduced progressively and reaches its lowest value at the last flashing chamber. The amount of the produced distillate decreases along the stages and consequently along with chambers. This is due to the increase of the heat of vaporization at lower saturation temperatures, and therefore, less amount of vapor is extracted from brine. Factually, the data in these figures also show that the higher the solar radiation the temperature is, the more the distillation rate rises since a larger amount of vapor can be extracted from salt water. The results also show that the higher the solar radiation the higher the flashed flow per chamber. Besides, the results also demonstrate that the higher the nanofluid concentration the higher the flashed flow produced during the flashing process compared to water as base fluid.

In thermodynamics, changes in the state or process of a system cannot be restored to its initial state by changes in the property of the system without the expenditure of energy [21]. An irreversible process increases the entropy of the system in question. The second law of thermodynamics can be used to determine the irreversibility of a process as per equation (16). In the thermodynamic process, the energy is lost to the surroundings in the form of Irreversible energy. However, the remaining amount of energy is defined as the Available Energy in the process [21]. This thermodynamic principle has been applied in the current study of the flashing chamber process and expressed in equations (15) and (16) to assess the lost and available energy. Figures 11 through 13 and 10 demonstrated the irreversibility and availability of solar radiation 1200 w/m2 during the flashing process at each stage. The results clearly showed that the irreversibility is reduced by using nanofluid at a higher concentration compared to water as a base fluid. Furthermore, the higher the concentration of the nanofluids the higher the availability at the last flashing chamber. However, the availability is progressively reduced at the last flashing chamber.

On the other hand, the results displayed the development of the flashed flow at different chambers and showed that the flashed flow is progressively reduced until reaching the lowest value at the last chamber. This is due to the increase of the heat of vaporization at lower saturation temperatures and therefore less amount of vapor is extracted from brine. As expected, the higher the concentration of the nanofluid the higher the amount of flashed flow produced.

Figure 16 shows the impact of solar radiation on the flashed flow, there is clear evidence that the higher the solar radiation the higher the flashed flow produced. Also, these figures show that nanofluid $Ai_2O_3$ produces the highest flashed flow among the nanofluids under investigation and water as the base fluid.

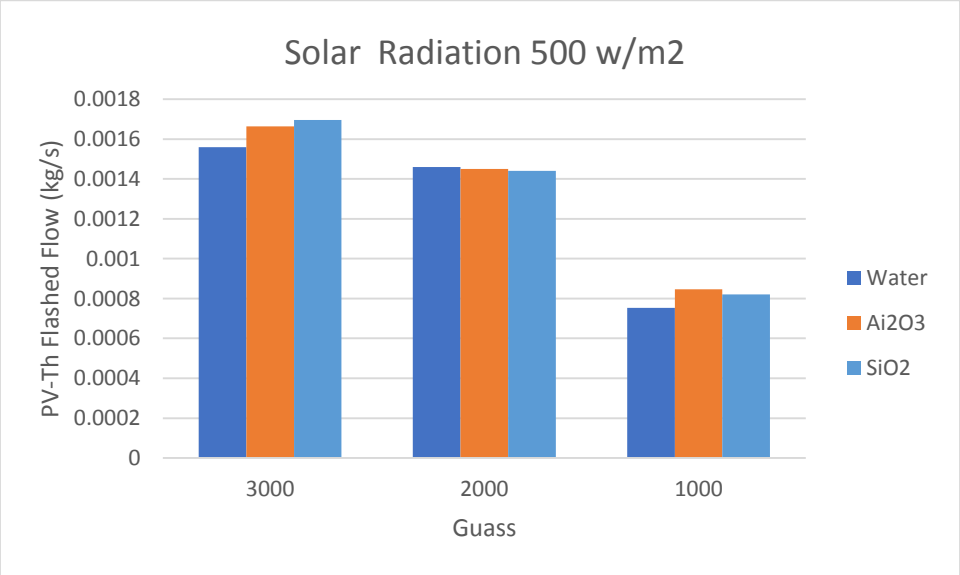


Figure 3 PV Thermal Flashed flow rate at different magnetic fields

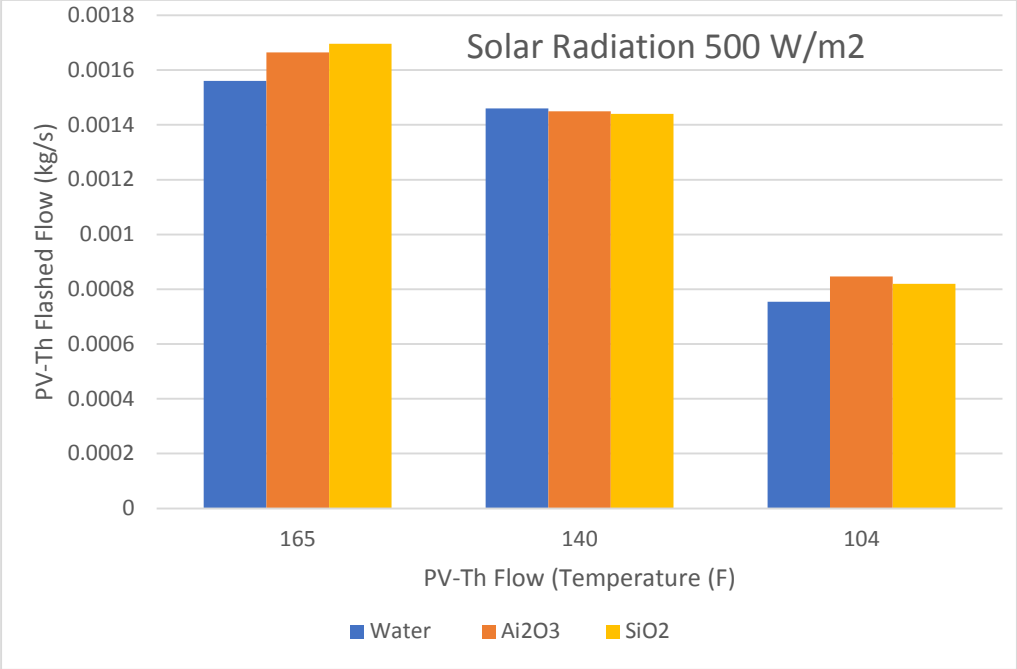


Figure. 4 PV Thermal Flashed flow rates and different temperatures

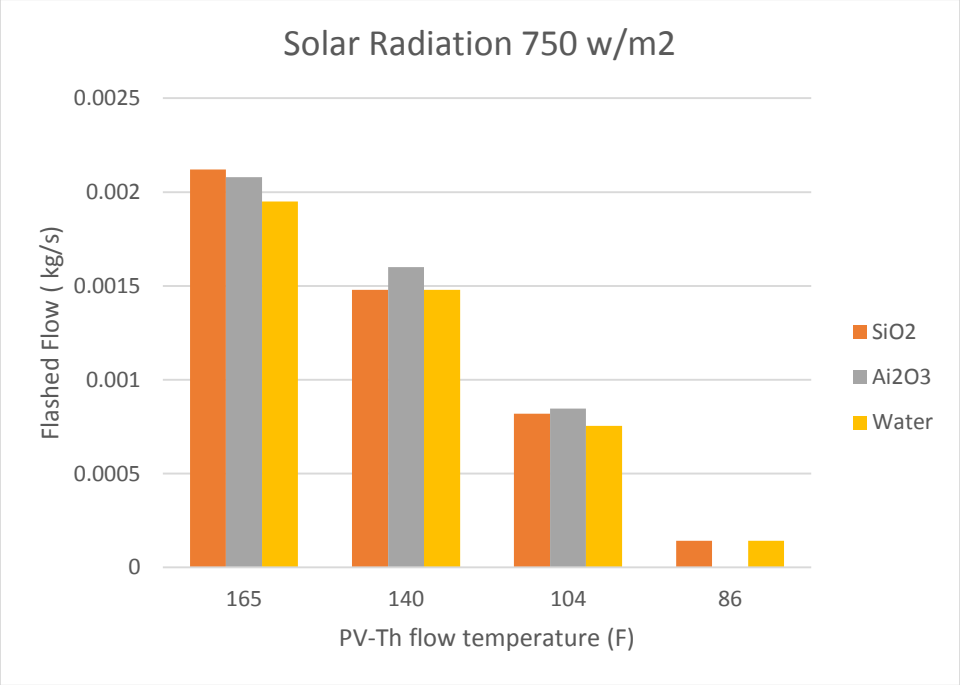


Figure. 5 Flashed flows at different temperatures

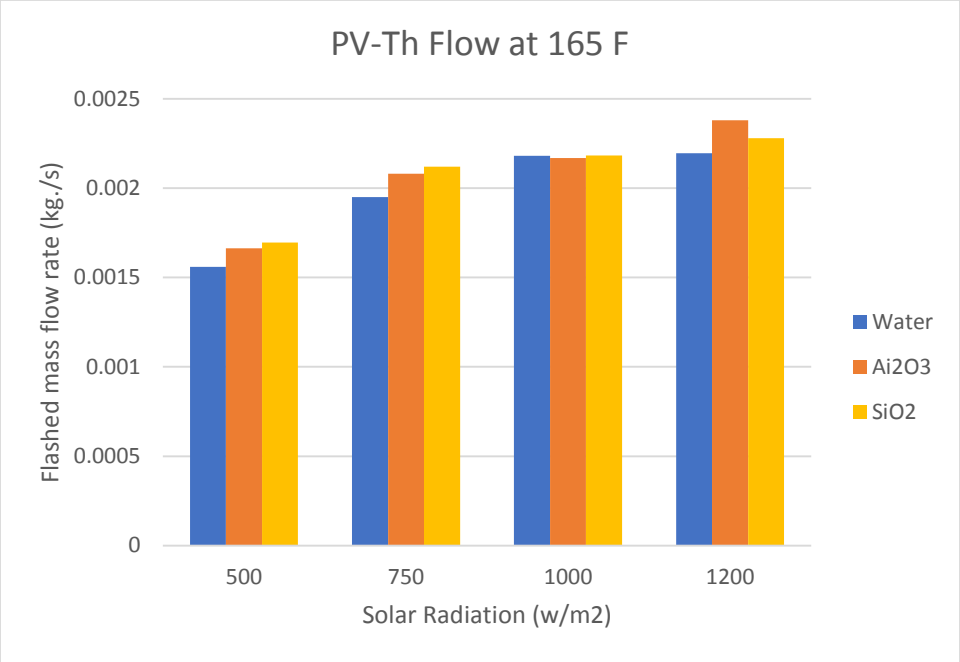


Figure. 6 Flashed flow and different solar radiations

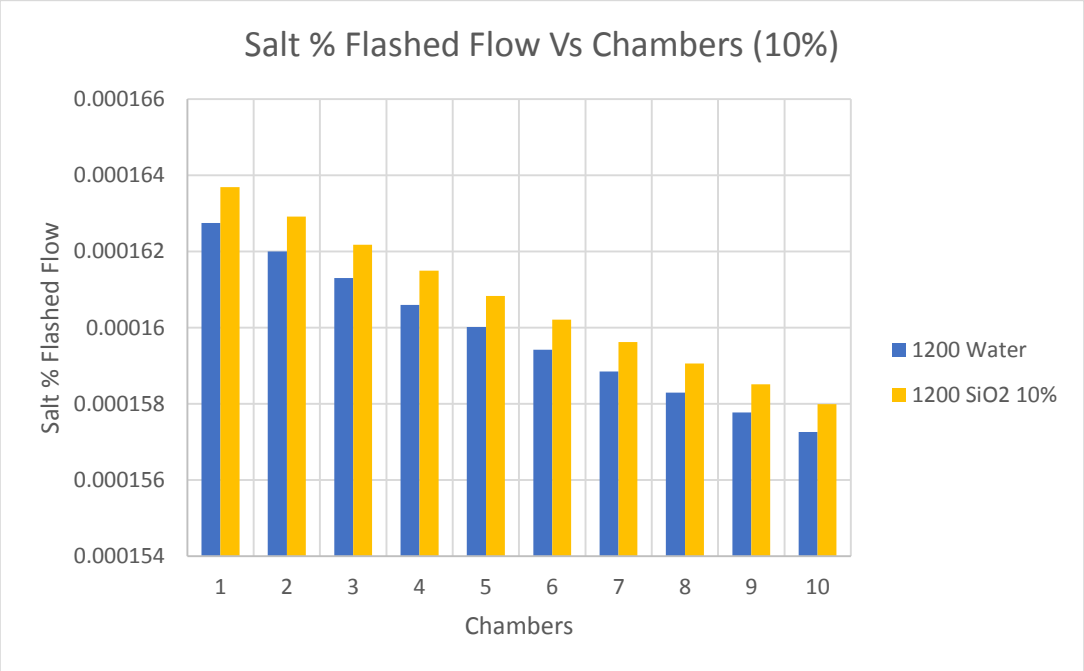


Figure. 7 Salt% flashed flow at 1200 w/m2

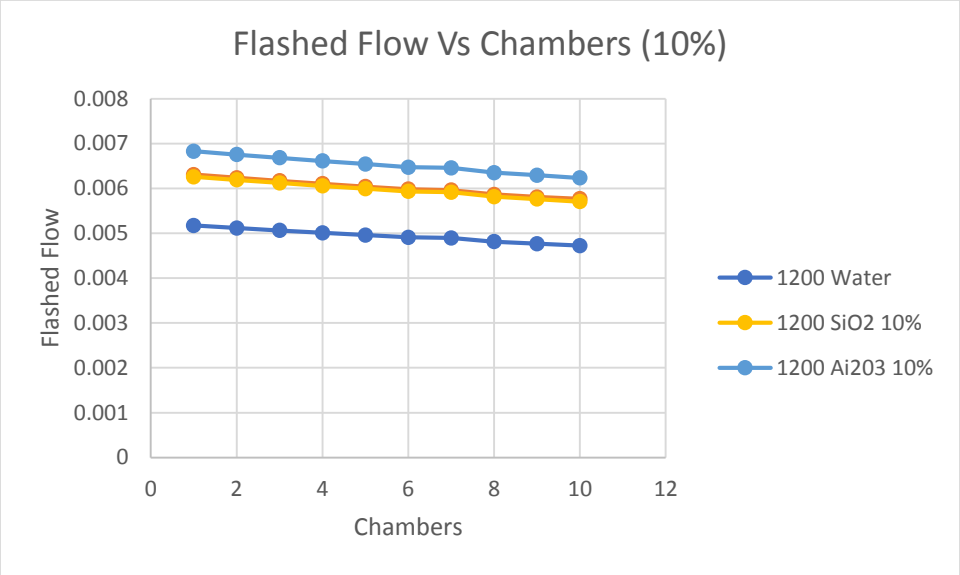


Figure. 8 Flashed flows (kg/s) at different chambers.

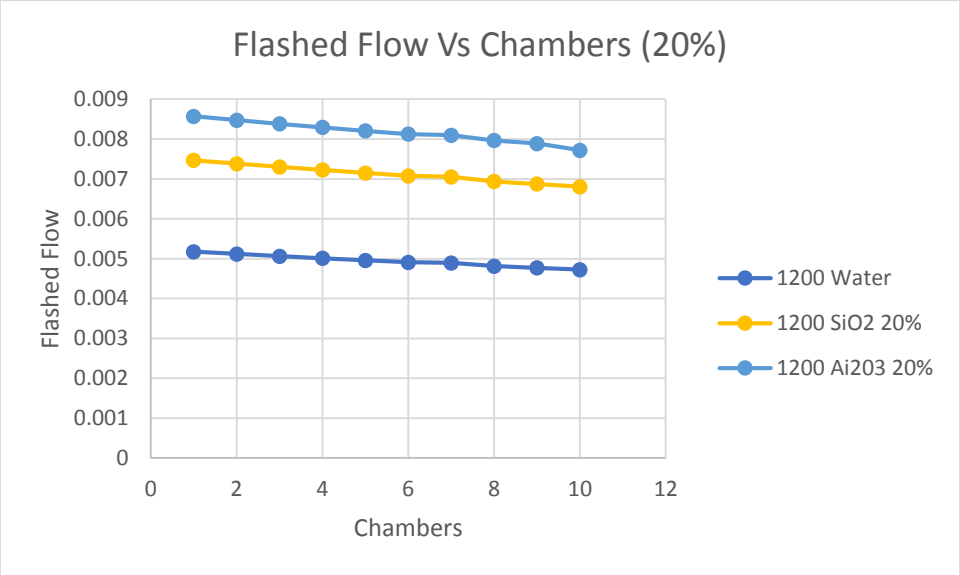


Figure. 9 Flashed flows (kg/s) at different concentrations

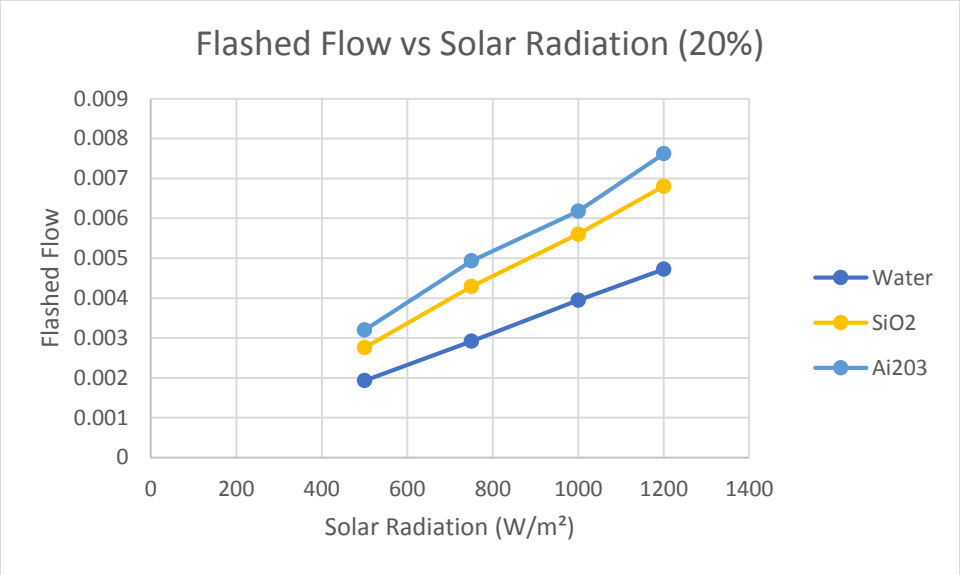


Figure. 10 Flashed flows (kg/s) at different solar radiations

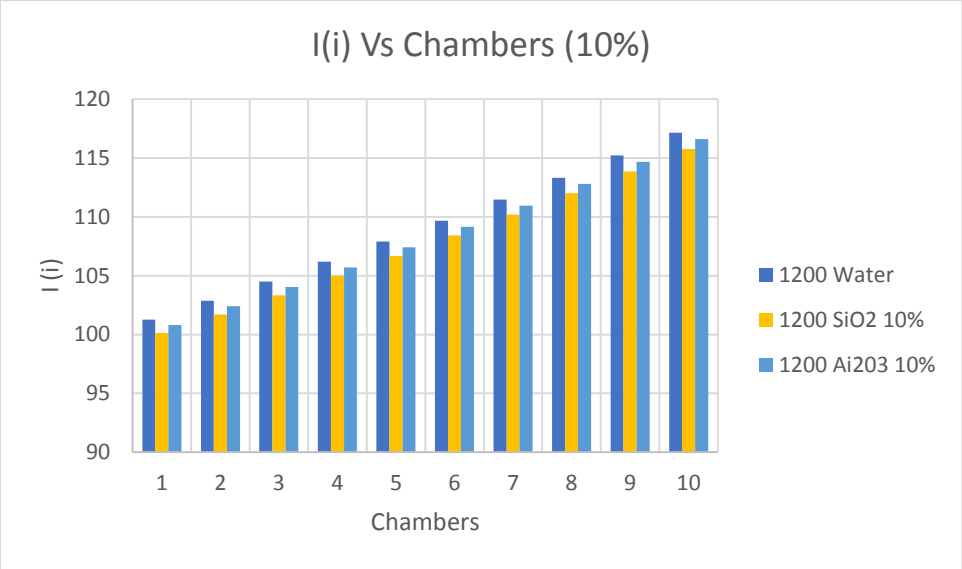


Figure. 11 Irreversibility (Btu/lb.) at different nanofluids

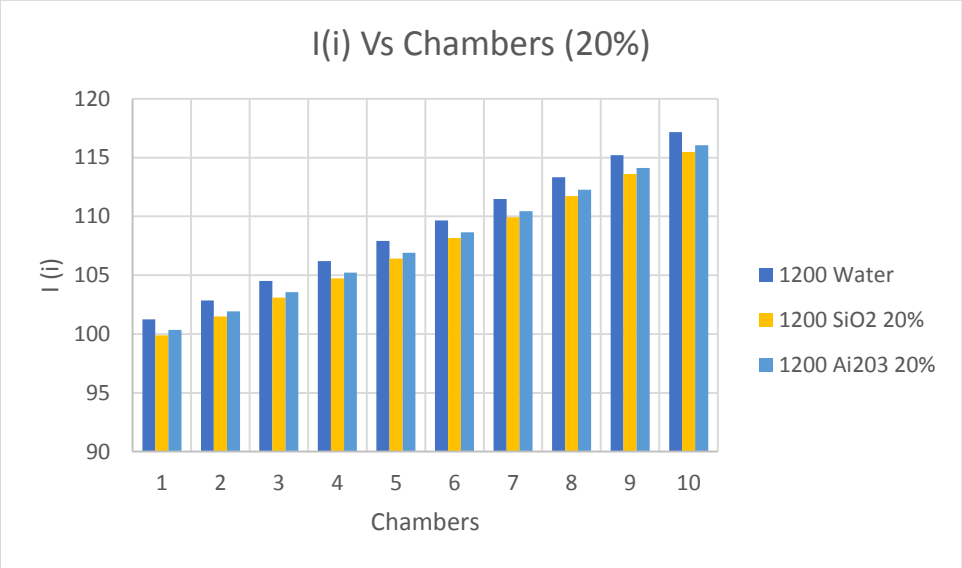


Figure. 12 Irreversibility (Btu/lb.) at different nanofluids

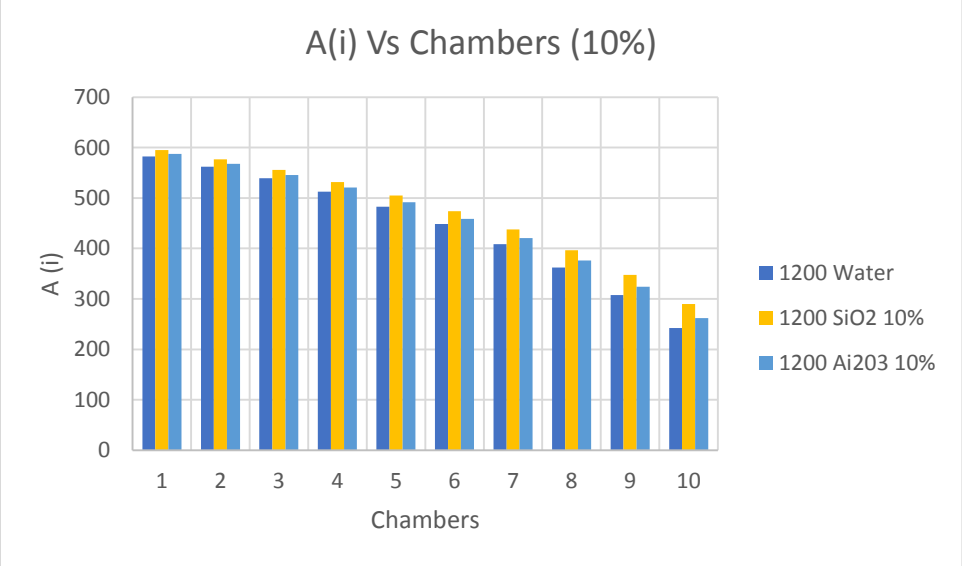


Figure. 13 Availability (Btu/lb.) at different nanofluids

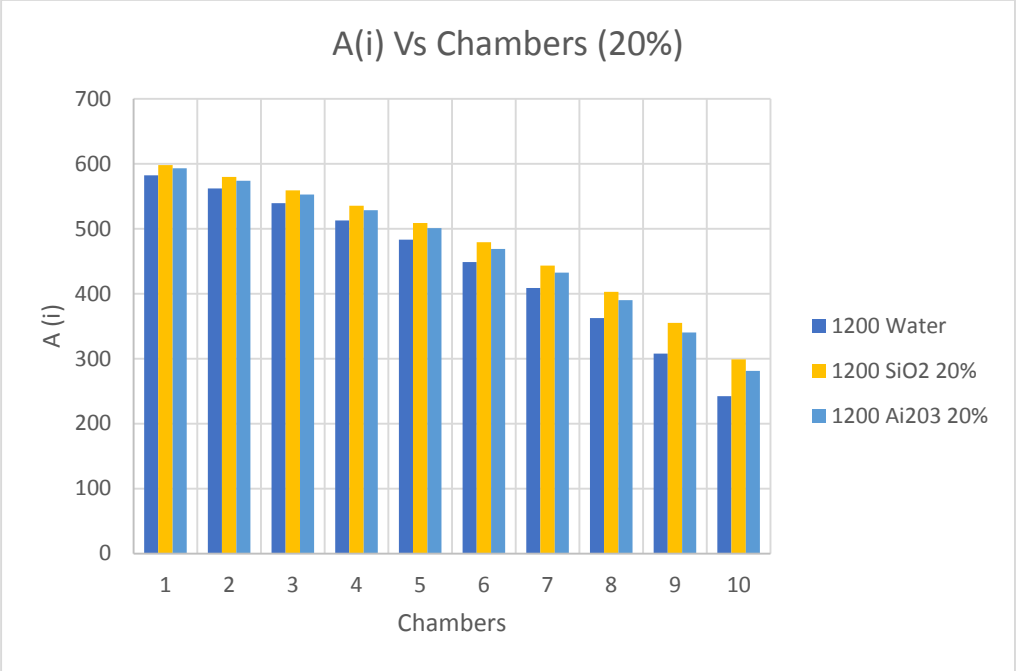


Figure. 14 Availability (Btu/lb.) at different nanofluids

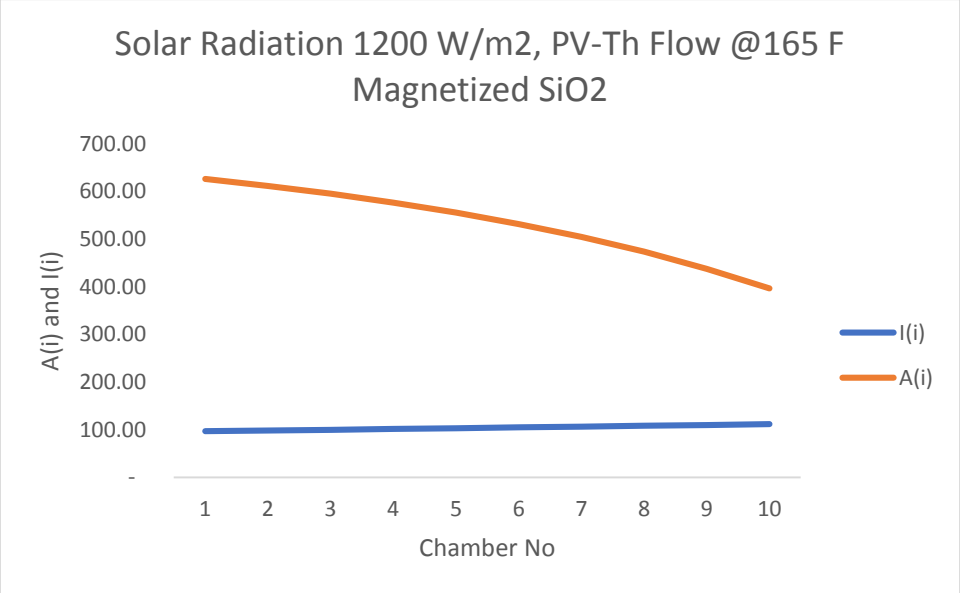


Figure 15 Comparison between the availability and irreversibility profiles

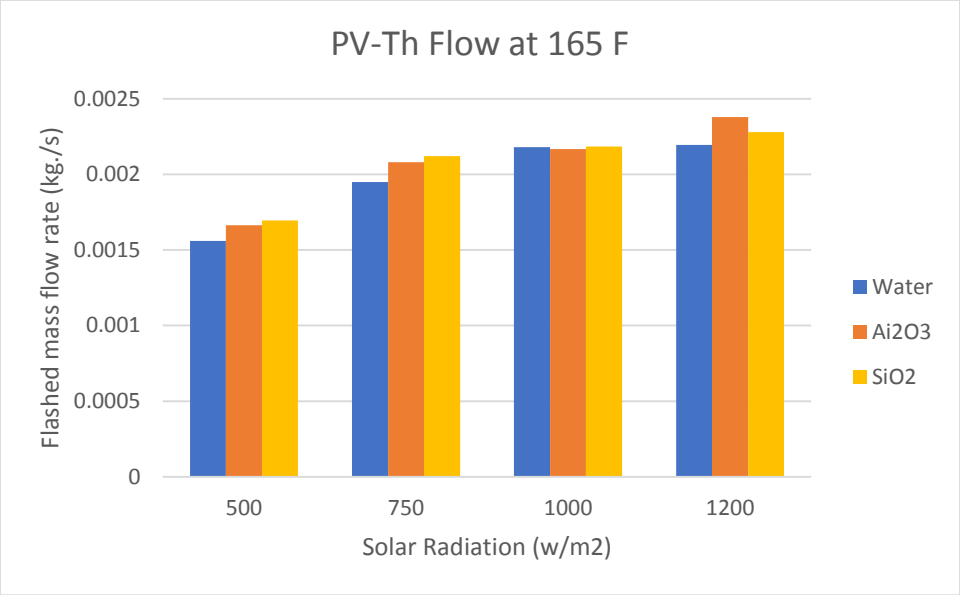


Figure 16 Flashed mass flow at different solar radiations.

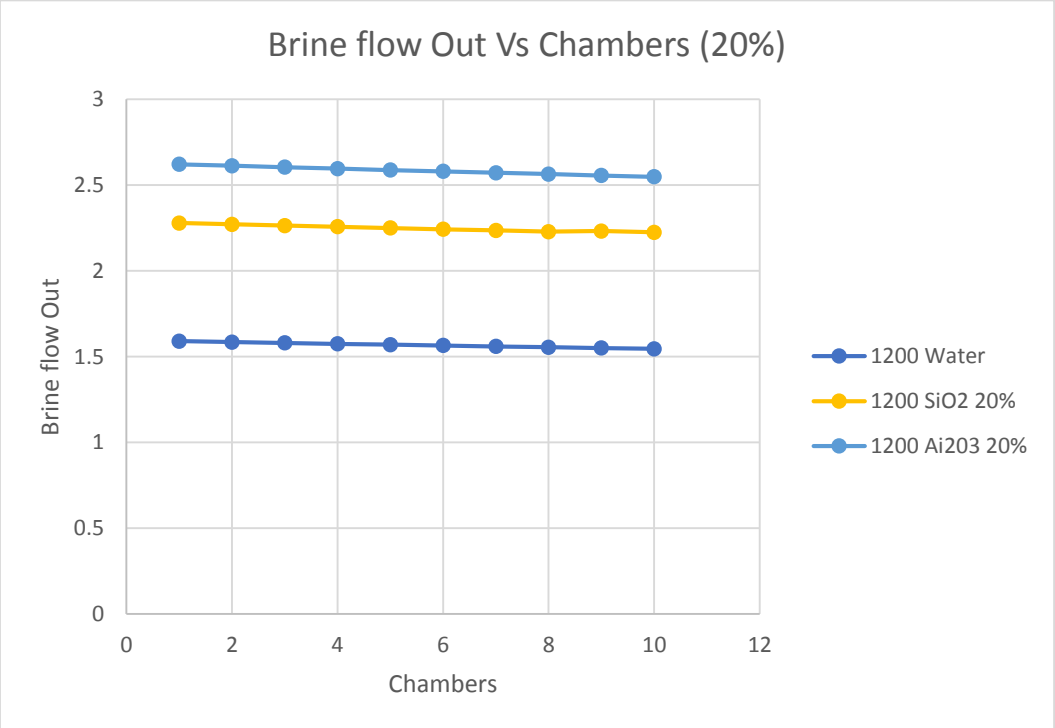


Figure .17 Brine profile across the flashing chambers

Figures 13 and 14 demonstrated clearly, that the irreversibility calculated by equation (16) is significantly influenced by the type of magnetized nanofluids used. As expected the irreversibility increases progressively across the chambers reaching a maximum at the last chamber. The highest irreversibility was experienced when water was used as heat transfer fluid while the lowest irreversibility was associated with the use of magnetized nanofluid $SiO_2$. This increase depends upon the type of nanofluid and its thermodynamic properties. Also, it appears that the concentration of the nanofluid does not have a significant effect not only on the changes of irreversibility across the various chambers but also during the flashing process.

It is clear that the availability determined by equation (15) diminishes progressively along with the flashing chambers and reaches the lowest value at the last chamber. And also the magnetized nanofluid concentrations have little effect on the availability during the flashing process. On the other hand, it can be observed from the results that the magnetized nanofluid $SiO_2$ has the highest availability across the flashing chambers among other nanofluids [32].

Finally, the brine outflow progressively decreased across the flashing chambers and in the last one. This was anticipated as at each chamber the amount of flashed vapor reduces the brine flow progressively along the chambers. It also appears that a higher concentration of the magnetized nanofluids increased the brine flows across the flashing chamber.

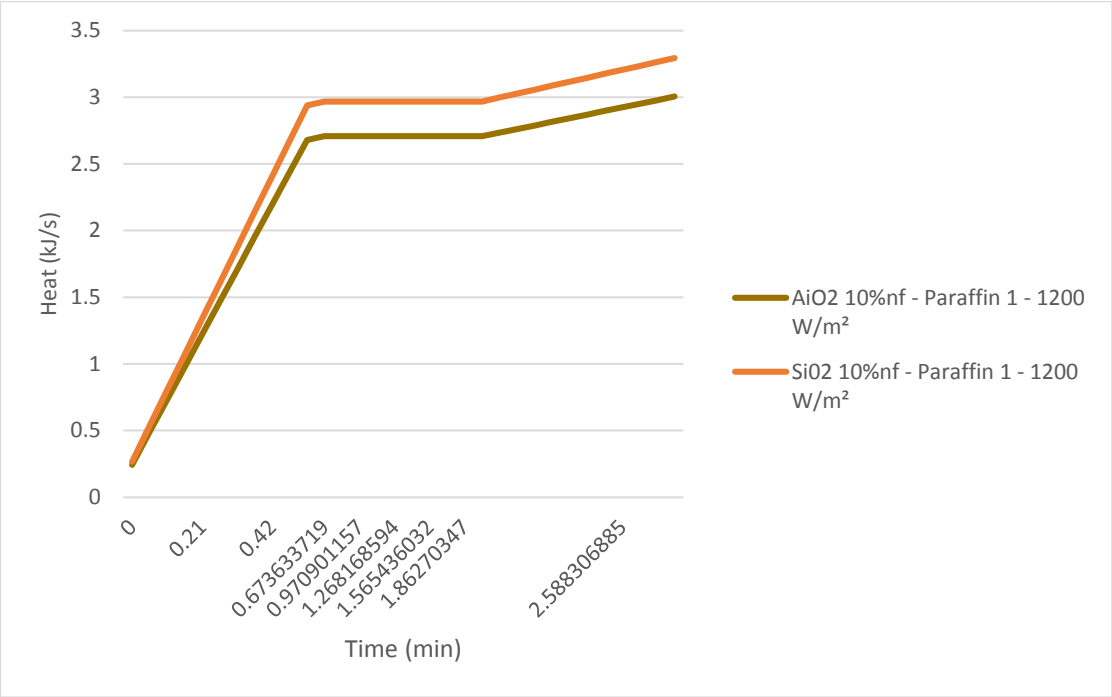


Figure 18 Thermal storage thermal energy during the charging phase at 1200 W/m2 and 10% concentration

Finally, it is worthwhile mentioning that lower nanofluids concentrations did not yield higher thermal capacities needed for the flashing process of the brine, therefore, 10% and 20% nanofluids concentrations were selected. Their impact on the pump power was taken into consideration while calculating the Availability and Irreversibility of the flashing process.

The results reported hereby on the magnetized nanofluids' behavior during the charging phase of the thermal storage process described in equations (17 through 24), using paraffin as Phase Change Material (PCM) at different concentrations demonstrated that a higher magnetized nanofluid concentration induces higher thermal energy build-up in the PCM. Also, the nanofluid $SiO_2$ has the highest thermal energy storage charge compared to the nanofluid $Ai_2O_3$ .

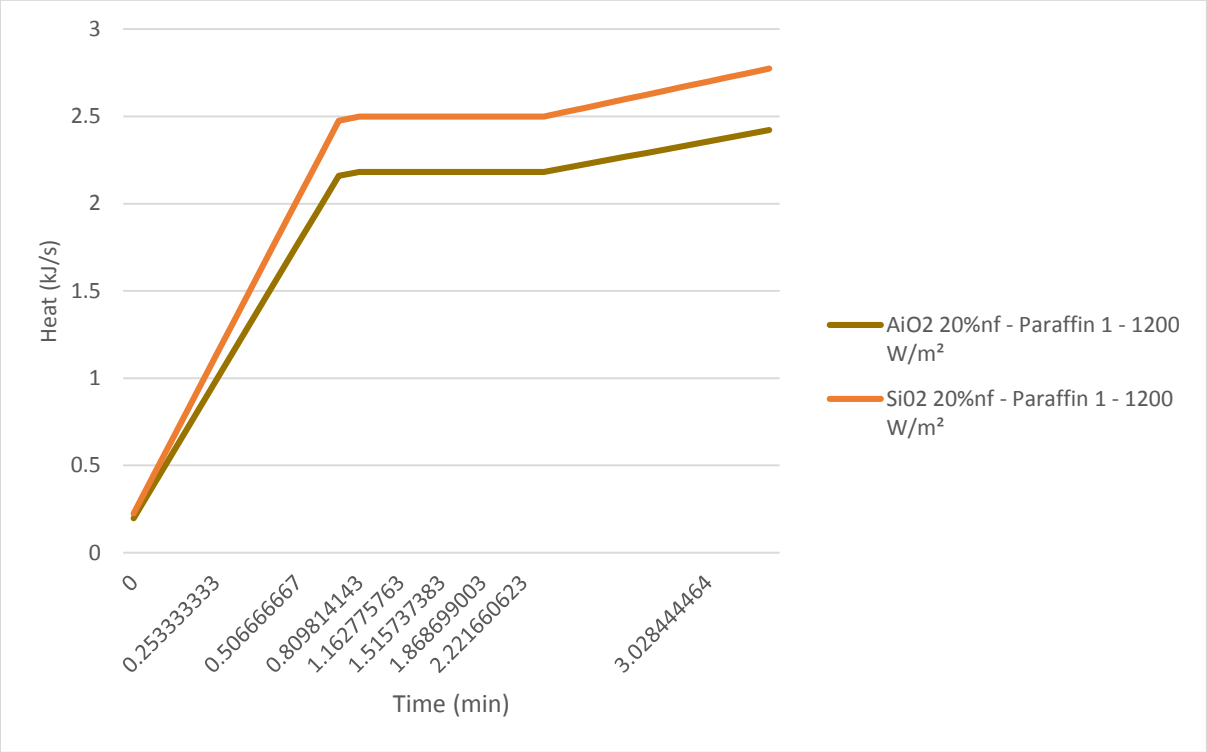


Figure 19 Thermal storage thermal energy during the charging phase at 1200 W/m2 and 20% concentration

**Model Validation**

The data published only by Nannaronea et al [7] was used to validate the numerical model in equations (1) through (16) and shown in Figure. 20. It was observed that the amount of the produced distillate saltwater decreases along the different stages progressively and consequently, the flash temperature and pressure decreased This is due to the increase of the heat of vaporization at lower saturation temperatures, and therefore, less amount of vapor is extracted from brine. The comparison clearly also shows that the model compared well with the data, however, the data was underpredicted by this model and that was attributed to the energy lost to the surroundings in the form of Irreversible energy during the flashing process taking place in each chamber and was not fully considered by the mass and energy balances built in the present model as can be seen in equation (16).

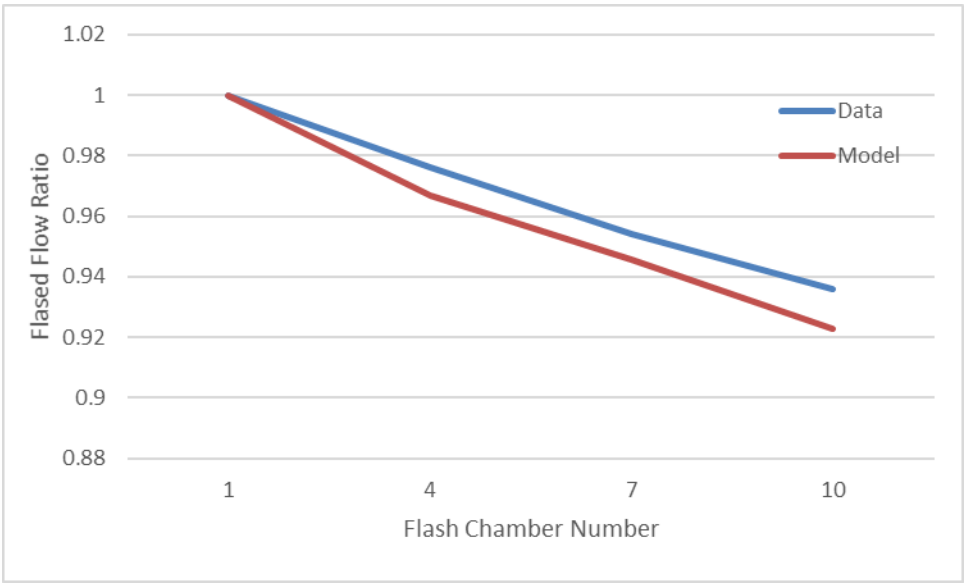


Figure 20 Comparison between model prediction and data [7].

## III. CONCLUSIONS:

This study presents a novel concept for solar desalination MSF implementing PV-Thermal solar panels and using hot heat transfer fluid, with magnetized nanofluids to drive the MSF process. A mathematical formulation describing solar desalination in the multistage flashing chamber process has been presented. It is developed using the mass and energy conservation equations written for the discrete control volume approach integrated with thermal and thermophysical properties of the water and magnetized nanofluids as heat transfer fluids. The nanofluids studied are $Ai_2O_3$ and $SiO_2$. The flashing process has been studied under various conditions including different solar radiations, brine concentrations, nanofluids concentrations, irreversibility, and availabilities at different temperatures. Solar radiation was taken between 500 W/m$^2$ and 1200 W/m$^2$. Nanofluids volumetric concentrations considered varied from 1% to 20%.

It was found that the higher the solar radiation the higher the flashed flow produced. Also, the irreversibility is reduced by using nanofluids at a higher concentration. The highest irreversibility was experienced when water was used as a base fluid and the lowest irreversibility was associated with nanofluid SiO2. The irreversibility increases depending on the type of nanofluid and its thermodynamic properties. Furthermore, the higher the concentration the higher the availability at the last flashing chamber. However, the availability is progressively reduced at the last flashing chamber. It was also observed that the nanofluid SiO2 has the highest availability among the other nanofluids and water-as-based fluids across the flashing chambers.

The results also added value to the research in thermal solar desalination through the use of solar energy, solar PV-Thermal panels with magnetized nanofluids as the driving force to the flashing evaporation process. This approach represents a step forward toward sustainability and reduction of the global warming effects. Finally, the predicted results were compared to limited experimental data in the literature and showed that the model fairly predicted the data under consideration. Finally, it is believed that future studies should investigate other nanofluids as well as different concentrations at different salt concentrations.

**ACKNOWLEDGEMENT:**
The research work presented in this paper was made possible through the support of TransPacific Energy, Inc.

**NOMENCLATURE**

$A_q$ the flow availability kj/kg
Cp the specific heat kj/kg k
$DT_{Stage}$ the stage temperature difference
$\Delta H_{evap}$ the stage enthalpy difference kJ/kg
G: Total Solar radiation incident on the PV module

H enthalpy kj/kg
$I_j$ Irreversibility kJ/kg
*m* mass flow rate kg/s
$Q_{in}$: Energy received due to solar irradiation,

$Q_{conv}$: Energy loss due to Convection

$Q_{elect}$: Electrical power generated.

*Sc* salt concentration, g/kg
$S_j$ is the entropy of the flashing process at each stage Kj/kg. K
$S_p$: Total area of the PV module

t: time

$T_j$ : Flashing chamber temperature, K
$T_{amb}$ Ambient temperature
Greek Symbols:
α thermal diffusivity
Φ nanoparticles' volumetric concentration.

ρ density, kg/m3

## References:


[1]. Ali M. El-Nashar, (2001), The economic feasibility of small solar MED seawater desalination plants for remote arid areas, Desalination 134 (2001) 173–186.

[2]. Mohamed A. Sharaf Eldean, (2011), Design and Simulation of Solar Desalination Systems, Thesis Submitted for the Ph.D. Degree in Energy Engineering to Faculty of Petroleum & Mining Engineering Suez Canal University, Egypt, 2011.

[3]. Hazim Mohameed Qiblawey, Fawzi Banat. (2008), Solar thermal desalination technologies. Desalination. 220 (2008) 633–644.

[4]. Fath H. (2000), desalination technology: The role of Egypt in the region. Fifth International Water Technology Conference, Alexandria, Egypt (2000).

[5]. Mohamed A. Eltawil, Zhao Zhengming, Liqiang Yuan. (2009), A review of renewable energy technologies integrated with desalination systems. Renewable and Sustainable Energy Reviews 13 (2009) 2245–2262.

[6]. Soteris A. Kalogirou, (2004), Solar thermal collectors and applications, Progress in Energy and Combustion Science 30 (2004) 231–295.

[7]. Parimal S. Bhambare, M. C. Majumder, Sudhir C. V. (2018) Solar Thermal Desalination: A Sustainable Alternative for Sultanate of Oman, International Journal of Renewable Energy Research, Vol.8, No.2, June 2018

[8]. Mahdi Shayanmehr, and Hamed Mahdavi, (2022), Mechanical modeling of a high-performance solar desalination system based on a three-step approach, Iranian Journal of Chemistry and Chemical Engineering, 10.30492/ijcce.2022.558036.5455

[9]. Alessandro Nannaronea, Claudia Torob, Enrico Sciubba, (2017), Multi-Stage Flash Desalination Process: Modeling and Simulation, Proceedings of Ecos 2017 - the 30th international conference on efficiency, cost, optimization, simulation and environmental impact of energy systems July 2-July 6, 2017, San Diego, California, USA, pages 1-12.

[10]. Hala Faisal Al-Fulaij, (2011), Dynamic Modeling of Multistage Flash (MSF)Desalination Plan, Thesis submitted for the degree of Doctor of Philosophy (Ph.D.) at University College London (UCL), July 2011.

[11]. A.O. Bin Amer, (2009), Development and optimization of ME-TVC desalination system, Desalination 249 (2009) 1315–1331.

[12]. Anum Iqbal, Mohamed Mahmoud, Enas Taha Sayed, Abdul Ghani Olabi, (2022), Evaluation of the nanofluid-assisted desalination through solar stills in the last decade, Journal of Environmental Management 277:111415, (2022), DOI: 10.1016/j.jenvman.2020.111415

[13]. Nigim, Tarek, (2017), Computational modeling of thermofluidic flashing in MSF desalination, A thesis submitted to the National University of Ireland as a fulfillment of the requirements for the Degree of Doctor of Philosophy, Department of Mechanical Engineering National University of Ireland, Galway, 2017.

[14]. A.E. Kabeel and Emad M.S. El-Said, (2014), Applicability of flashing desalination technique for small scale needs using a novel integrated system coupled with nanofluid-based solar collector, Desalination 333 (2014) 10–22.

[15]. S. Sami, (2020), Study of the Impact of PV-Thermal and Nanofluids on the Desalination Process by Flashing, Appl. Syst. Innov. 2020, 3, 10; doi:10.3390/asi3010010 www.mdpi.com/journal/asi.

[16]. Garg, Kapil & Khullar, Vikrant & Das, Sarit K. & Tyagi, Himanshu, (2018), Performance evaluation of a brine-recirculation multistage flash desalination system coupled with nanofluid-based direct absorption solar collector," Renewable Energy, Elsevier, vol. 122(C), pages 140-151.

[17]. D.J. Yang, Z.F. Yuan, P.H. Lee, and H.M. Yin, (2012), Simulation and experimental validation of heat transfer in a novel hybrid solar panel, International Journal of Heat and Mass Transfer 55 (2012) 1076-1082

[18]. B. Lalovi, z. Kiss, H.A. Weakliem (1986), "Hybrid amorphous silicon photovoltaic and thermal solar-collector", Sol Cells 19, PP 131–138.

[19]. Kapil Garg, Sarit Kumar, Vikrant Khullar, Himanshu Tyagi (2022), Application of Nanofluid-Based Direct Absorption Solar Collector in Once-Through Multistage Flash Desalination System, DOI: 10.1007/978-981-13-3302-6_16, Advances in Solar Energy Research, January 2019.

[20]. S. Sami, (2019), Prediction of Performance of a Novel Concept of Solar Photovoltaic-Thermal Panel and Heat Pipe Hybrid System, International Journal of Modern Studies in Mechanical Engineering (IJMSME) Volume 5, Issue 1, 2019, PP 1-26, ISSN 2454-9711 (Online), DOI: http://dx.doi.org/10.20431/2454-9711.0501001.

[21]. S. Sami and C. Campoverde; (2018), Dynamic Simulation and Modeling of a Novel Combined Hybrid Photovoltaic-Thermal Panel Hybrid System, International Journal of Sustainable Energy and Environmental Research 2018 Vol. 7, No. 1, pp. 1-23.

[22]. S. Sami and E. Marin, (2019), Modelling and Simulation of PV Solar-Thermoelectric Generators using Nano Fluids, International Journal of Sustainable Energy and Environmental Research, IJSEER, 2019 Vol. 8, No. 1, pp. 70-99, DOI: 10.18488/journal.13.2019.81.70.99.

[23]. Mohammad A. Hamdan, Anas M. Al Momani, Osama Ayadi, Ahmad H. Sakhrie, and Francisco Manzano-Agugliaro, (2021) Enhancement of Solar Water Desalination Using Copper and Aluminum Oxide Nanoparticles, Water 2021, 13(14), 1914; https://doi.org/10.3390/w13141914

[24]. Allen, C., (2015). Magnetic field enhancement thermal conductivity analysis of magnetic nanofluids. MSc, the University of Texas at Arlington.

[25]. Ali H.A. Al-Waelia, Miqdam T. Chaichanb, Hussein A. Kazemc, K. Sopiana, Javad Safaeia (2018), Numerical study on the effect of operating nanofluids of the photovoltaic thermal system (PV/T) on the convective heat transfer, Case Studies in Thermal Engineering 12 (2018) 405–413, https://doi.org/10.1016/j.csite.2018.05.011.

[26]. Moran, John (2008). Fundamentals of Engineering Thermodynamics, p. 220. John Wiley & Sons, Inc., USA. ISBN 978-0-471-78735-8.

[27]. S. Sami, (2019) «Modelling and Simulation of Performance of Nanofluids in PV-Thermal Solar Panel Collectors», RA JOURNAL OF APPLIED RESEARCH, ISSN: 2394-6709 (Online), DOI: https://doi.org/10.31142/rajar/v5i1.07

[28]. S. Sami, (2019) «Prediction of Performance of a Novel Concept of Solar Photovoltaic-Thermal Panel and Heat Pipe Hybrid System», International Journal of Modern Studies in Mechanical Engineering (IJMSME) Volume 5, Issue 1, 2019, PP 1-26, ISSN 2454-9711 (Online), DOI: http://dx.doi.org/10.20431/2454-9711.0501001

[29]. Valery Ya. Rudy and Andrey V. Minakov, Thermophysical properties of nanofluids, The European Physical Journal E volume 41, Article number: 15 (2018).

[30]. Sami, S., and Copado, O. (2016) "Numerical Analysis of Integrated Phase Change Material in Solar Water Heating Systems", IJEPE, International Journal of Energy and Power Engineering, Volume 5, No 3, p 105 - 112, 2016.

[31]. Sami, S., and Zaratain, J. (2016) "Thermal Analysis and Modeling of Thermal Storage in Solar Water Heating Systems", IJEPE, International Journal of Energy and Power Engineering, Volume 5, No 2, p 48-59, 2016.

[32]. S. Sami, (2023) "Investigation of Low-Temperature Desalination Process by Flashing, PV-Thermal, Thermal Storage, and Magnetized Nanofluids", SSRG International Journal of Thermal Engineering Volume 9 Issue 1, 1-11, Jan-Apr 2023, ISSN: 2395-0250/ https://doi.org/10.14445/23950250/IJTE-V9I1P101 © 2023 Seventh Sense Research Group (2023)